Session 3P8b
Media

Lithium Ferrites for Phase Shifter

F. Q. Yuan
Southwest Jiaotong University, China

The dramatic development of satellite television has attracted people's profound attention on the receipt of satellite television programs by motion carriers such as trains and long distance buses. Meanwhile, to develop the remote education system in our nation so that the border areas can receive satellite television programs, we have conducted research on flat plate phase array antenna system of autotrack synchronous communication satellite. However, the development of this system is dependent greatly on the quality and materials of component. Therefore, we have conducted deep discussion on materials of phase shifter.

Using standard ceramic technique on pure oxide: ZNO, TiO_2, SnO_2, Fe_2O_3 and carbonate Li_2CO_3 as raw materials, we prepared the $Li_{0.5(1-y)}Zn_yFe_{2.5(1-0.2y)}O_4$ Lithium ferrites (with $y = 0$, 0.1, 0.16, 0.25, 0.28) and Kuband Ferrite phase shifter materials $Li_{0.625}Zn_{0.1}Ti_{0.25}Sn_{0.1}Fe_{1.925}O_4$. Flowing-oxygen begins at 800°C to 900°C and the pressure of wet pressing is about 9.8×10^{11} Pa. The temperature of flowing-oxygen sintering is from 850°C to 1050°C and some beneficial materials: Bi_2O_3, NiO, Co_2O_3 and $MnCO_3$ are added.

Through the analysis of the X-ray diffraction, it is shown that all generating materials are monophasic Lithium ferrites. The test results of $Li_{0.625}Zn_{0.1}Ti_{0.25}Sn_{0.1}Fe_{1.925}O_4$ ferrite at 300 K are tabulated in Table 1. Figure 1 shows the relation between specific saturation magnetization of $Li_{0.625}Zn_{0.1}Ti_{0.25}Sn_{0.1}Fe_{1.925}O_4$ and temperature. Figure 2 gives the relation between saturation magnetization of $Li_{0.5(1-y)}Zn_yFe_{2.5(1-0.2y)}O_4$ and substituent y.

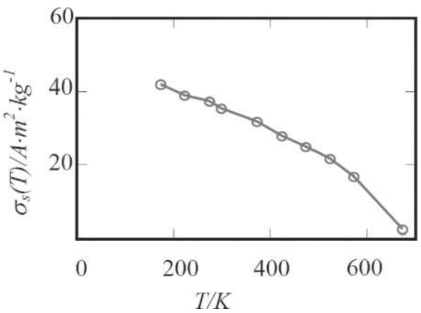

Figure 1: Relation between specific saturation magnetization σ_s and temperature T.

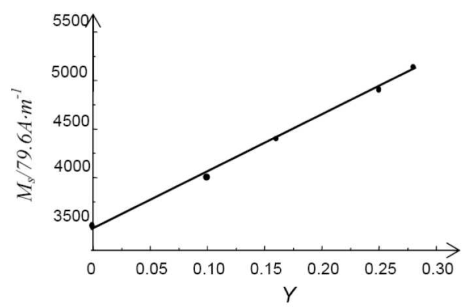

Figure 2: Relation between magnetization M_s and substituent y.

Table 1: Test results of $Li_{0.625}Zn_{0.1}Ti_{0.25}Sn_{0.1}Fe_{1.925}O_4$ ferrite at 300 K.

Sample	g	R_r	H_c	ρ	ε'	$tg\delta_\varepsilon$	M_s	ΔH	T_c
$Li_{0.625}Zn_{0.1}Ti_{0.25}Sn_{0.1}Fe_{1.925}O_4$	2.0	0.9	0.7	4.5	16.2	4.2	2060	285	678

It is shown from above analysis that magnetic dipole moment of ferrite $Li_{0.5(1-y)}Zn_yFe_{2.5-0.2y}O_4$ is equal to the magnetic dipole moment difference of Fe^{3+} on B sites and Fe^{3+} on A sites, which is to say, the number of Bohr magnetons per unit molecular formula in $(Zn_yFe_{1-0.5y})$ $[Li_{0.5(1-y)}Fe_{1.5}]O_4$ ferrite is $n_B = 1.5-1+0.5y = 0.5(1+y)$, an increase in y will increase n_B, therefore, saturation magnetization increase linearly with the increase of substituent y. However, the saturation magnetization is decreased when y is increased to such an extent that the super-exchange interactions of Fe^{3+} on A and B sites become weak owing to excessive concentration of nonmagnetic Zn^{2+} ions, leading to a incline of Fe^{3+} magnetic dipole moment and a partial spinflip.

*This work was supported by National Science Foundation of P. R. China. Grant No. 60371017.

A Novel Thin Microwave Absorber Based on the Concept of Equivalent Transformation Method of Material Constant

Y. Kotsuka and K. Shimodaira
Tokai University, Japan

The authors have thus far proposed the effective methods of changing and improving the matching characteristics of a single magnetic EM wave absorber [1–3]. These methods based on not by adjusting the processing conditions to produce a new magnetic material such as ferrite, but by applying static magnetic fields to a magnetic absorber, by adjusting the geometrical shape of it, and by attaching conductive patterns to the surface of absorbers etc. We have called these methods "Equivalent Transformation Method of Material Constant (ETMMC)" [4]. To change the matching frequency characteristic toward higher frequency regions from the original one, small holes are punched out in a magnetic absorber [2]. Secondly, to shift the matching frequency characteristic toward low frequency regions, conductive patterns are attached periodically to the surface of a ferrite absorber [3, 4].

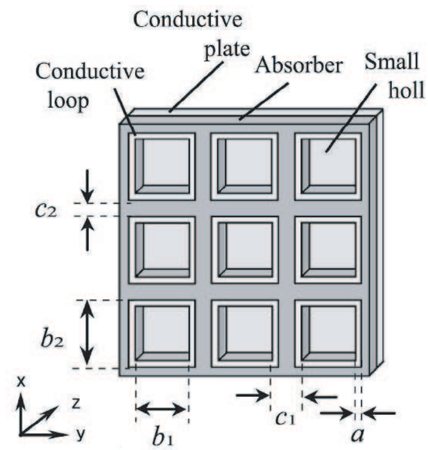

Figure 1: Fundamental construction of present absorber.

In this paper, a thin and light weight EM-wave absorber is newly proposed. It becomes possible to merge both the competing characteristics by means of punching out small holes in the magnetic absorber and by attaching periodical conductive patterns to the surface of it as shown in Fig. 1. The question is what kinds of matching frequency characteristic are obtained by combining both the competing characteristics of changing the matching frequency toward high or low frequency regions. The detailed matching characteristics of the present absorber are investigated based on FDTD analysis. The matching mechanism is clarified from input admittance chart viewpoints. Consequently, a new thin and light weight microwave absorber can be realized with the thickness of 2.0 mm at the frequency from 2.45 GHz to above 6 GHz and light weight due to small holes occupying 55% of the area to carbonyl absorber.

REFERENCES

1. Kotsuka, Y., et al., "Fundamental investigation on a weakly magnetized absorber," *IEEE Trans. EMC*, Vol. 42, No. 2, 116–124, May 2000.
2. Amano, M. and Y. Kotsuka, "A method of effective use of ferrite for microwave absorber," *IEEE Trans. MTT*, Vol. 51, No. 1, 238-245, Jan. 2003.
3. Amano, M. and Y. Kotsuka, "A novel microwave absorber with surface-printed conductive line patterns," *IEEE MTT-S Int. Microwave Symp. Dig.*, 1193–1196, Jun. 2002.
4. Kotsuka, Y., "EM-wave absorbers based on equivalent transformation method of material," *Constant, Proc. of the 2004 IEICE Society Conference*, BS-1-1, S-1-S2, Sep. 2004.

A Study of RF Absorber for Anechoic Chambers Used in the Frequency Range for Power Line Communication System

K. Shimada and K. Ishizuka
Riken Eletech Corporation, Japan

M. Tokuda
Musashi Institute of Technology, Japan

Abstract—Power line communication (PLC) system is spreading as a new communication system without providing new infrastructure for network communication. However, It is needed to investigate the EMI problem caused by PLC, and it is often tested in an anechoic chamber and an open area test site (OATS). The semi anechoic chamber lined ferrite tiles used for EMC testing is not generally designed in the frequency range from 2 MHz to 30 MHz used for PLC system. This paper presents characteristics of conventional ferrite absorber which are used for a semi anechoic chamber (SAC) and site attenuation of the semi anechoic chamber in the frequency range used for PLC system.

1. Introduction

Recently, power line communication (PLC) system is spreading as convenient communication without providing new infrastructure for network communication. PLC system is using utility-owned power lines in the low-voltage mains grid to provide broadband Internet access in areas that are mostly residential. PLC uses unshielded, low-voltage power line distribution cables inside and outside of buildings as transmission media with high speed rates. Because PLC system uses the frequency range from 2 MHz to 30 MHz in order to communicate information, it becomes a subject of discussion to influence other electrical or electronic device. Therefore RF emissions from PLC system have been investigated in an anechoic chamber or an open area test site (OATS). Ferrite absorber with thickness from about 6 mm to 7 mm without some kind of pyramidal absorbers is used for 3 m or compact anechoic chamber (CAC), because the ferrite absorber has excellent absorption in the frequency range from 30 MHz to 1 GHz. In this paper, we discussed the characteristics of conventional ferrite absorber which is used for a 3 m or a CAC from 2 MHz to 30 MHz utilized for PLC system. Site attenuation characteristics of the conventional 3 m anechoic chamber were investigated.

Figure 1: Semi anechoic chamber lined ferrite tiles. (Ferrite tiles are installed back of the white interior finishing panel. Pyramidal ferrite absorbers are installed back of the black color rea).

2. Characteristics of Ferrite Absorber

2.1. Measurement Method

The Reflection characteristics, relative permittivity and relative permeability of ferrite absorbers were measured using the coaxial line with a diameter of 39 mm (The 39 D Coax.) in Figure 2, and the square coaxial line with a section of 300 mm × 300 mm (The Square Coax.) in Figure 3. The 39 D Coax is used for measurement complex permittivity and permeability. In this paper, it was used to measure characteristics of ferrite material without small gaps. It is well known that minute air gaps between ferrite tiles reduce absorption of ferrite absorber, and the Square Coax is able to evaluate the reflection of ferrite tiles including the air gaps. This measurement procedure of the Square Coax is same way as the 1.8 m × 1.8 m Large Square Coax which had been developed and presented [1]. The Square Coax is an outer conducting line with a section of 302 mm × 302 mm and an inner conducting line with a section of 98 mm × 98 mm, and eight pieces of ferrite tiles were arranged. A special feature is to set two ports in order to measure full complex S parameter (S11, S22 and S21) of a test sample, and it is possible to calculate complex permittivity and permeability from the measured S parameter of the test sample. As it is well known, it is very important to know the complex permittivity and permeability. Because the characteristics impedance of the Square Coax was about 60 Ω, there was impedance mismatching between a 50 Ω coaxial cable and a port of the Coax. To solve this mismatching problem, a serial resistance was inserted at the end of inner conducting line, and it could reduce inner reflection. On the other hand, the mismatching at the port of viewpoint from outside increased by the inserted serial resistance. The complex S parameters which removed the redundant reflections are driven by quotation (1), (2), and (3).

$$S11_{cor} = \frac{S11_{sample} - S11_{air}}{1 - S11_{air}} \quad \mathrm{RPR_{S11}} \tag{1}$$

$$S22_{cor} = \frac{S22_{sample} - S22_{air}}{1 - S22_{air}} \quad \mathrm{RPR_{S22}} \tag{2}$$

$$S21_{cor} = \frac{S21_{sample}}{S21_{air}} \tag{3}$$

Where

$$\mathrm{RPR_{S11}} = e^{J\cdot\frac{2\pi\cdot 2(EL_{s11}-d)}{\lambda}} \tag{4}$$

$$\mathrm{RPR_{S22}} = e^{J\cdot\frac{2\pi\cdot 2\cdot EL_{s22}}{\lambda}} \tag{5}$$

$$\mathrm{RPR_{S21}} = e^{J\cdot\frac{2\pi\cdot d}{\lambda}} \tag{6}$$

Where
d: Thickness of test sample
λ: Wave length
$\mathrm{EL_{S11}}$: Electric Length between the calibration point of port 1 and the sample set point
$\mathrm{EL_{S22}}$: Electric Length between the calibration point of port 2 and the sample set point

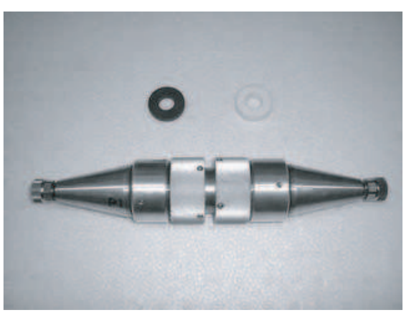

Figure 2: The 39D Coax and test sample.

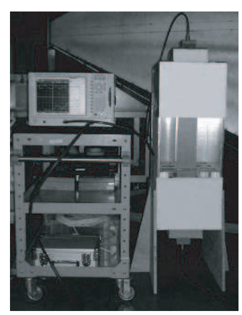

Figure 3: The 300 Square Coax.

2.2. Fundamental Characteristics of Ferrite Absorber

At first the fundamental characteristics of the Ni–Zn–Cu ferrite absorber with 6.3 mm thick was investigated below 30 MHz, in order to confirm the characteristics which is influenced by minute air gaps between ferrite tiles. The 39 D Coax and the Square Coax were each used for obtaining the fundamental characteristics of without or with the influence of minute air gaps. Figure 4 shows the shape of test sample for 39 D Coax, and Figure 5 shows the eight piece of ferrite tiles are inserted in the Square Coax.

Figure 6 shows chart of the reflectivity of conventional ferrite absorber which was measured using the 39 D Coax. In this chart, this ferrite absorber does not have sufficient absorbing characteristics in the frequency range from 3 MHz to 30 MHz used for PLC system. The absorbing characteristics of eight piece of ferrite tile including minute air gaps were reduced compared from the measured data of ferrite absorber with no air gap.

These air gaps were not artificially given between ferrite tiles, ferrite tiles were arranged to keep minimum air gaps. The complex permittivity and permeability are shown in Figures 7 and 8, and the value of the imaginary permeability which is loss paragraph is reduced by minute air gaps.

Figure 4: Test sample for 39D Coax.

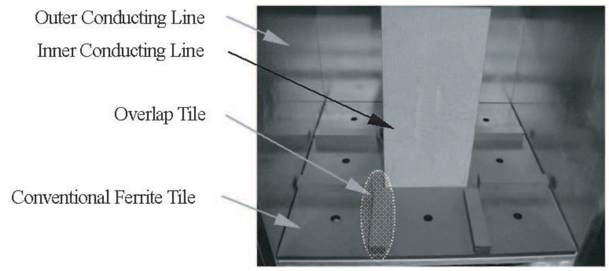

Figure 5: Arrangement of Ferrite Tiles in the 300 Square Coax.

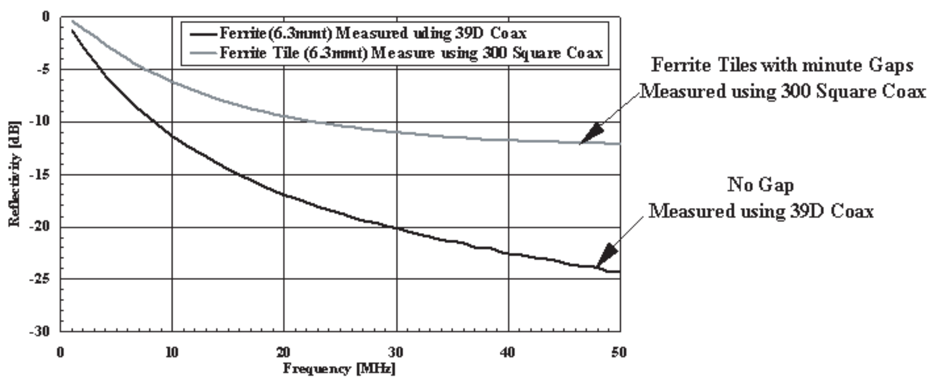

Figure 6: Measured permittivity and permeability of ferrite absorber with short end.

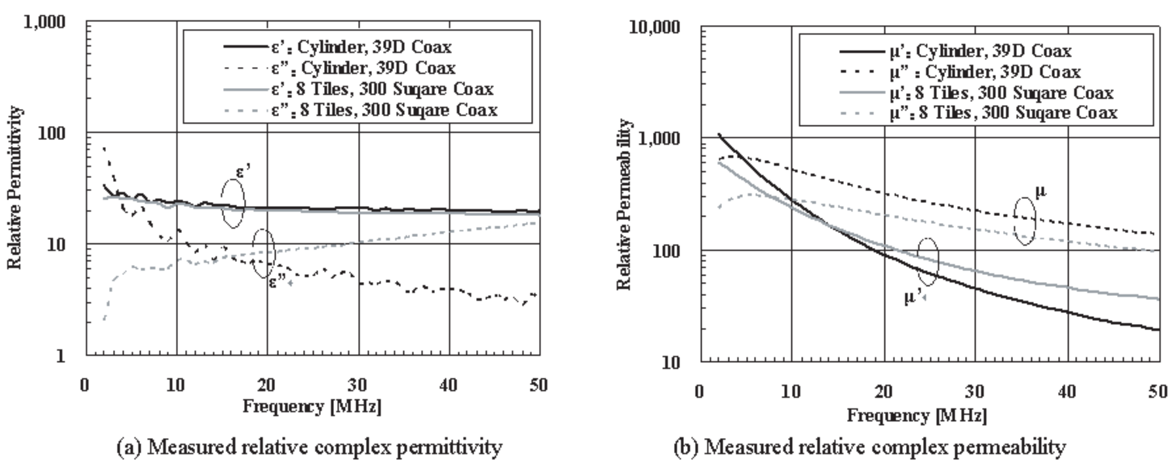

Figure 7: Measured permittivity and permeability of ferrite absorber. (Compare of 39 D and 300 Square Coax.)

2.3. Various Measurement Results

The following methods were investigated in order to improve the absorption of the ferrite tiles with minute air gaps.

(1) Change the thickness of the ferrite.
(2) Put overlap tile onto the joint between ferrite tiles as shown in Figure 5.
(3) Combine a carbon material board on the ferrite absorber.

Figure 8 shows the reflectivity of the ferrite tiles with a thickness of 6.3, 8, 10 and 12 mm thick. The reflectivity became to reduce with to thicken the ferrite below 15 MHz, and it became larger over 10 mm thick in the frequency range above 15 MHz. To put overlap tile onto the ferrite tile reduced the reflectivity of the ferrite in Figure 9.

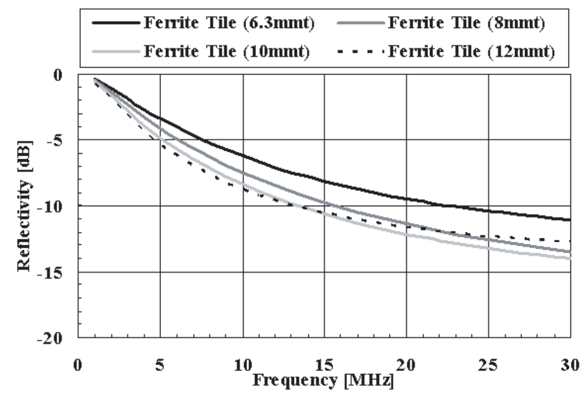

Figure 8: Relation reflectivity and thickness of ferrite.

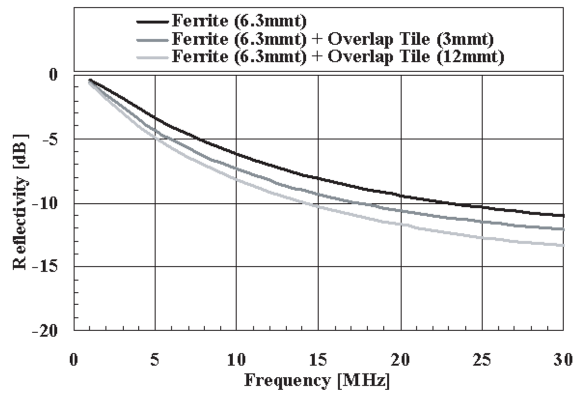

Figure 9: Reflectivity of using overlap tile .

It was studied that combining carbon material was reduced the reflectivity of the conventional ferrite from 3 MHz to 30 MHz used PLC system. Figure 10 shows the relative complex permittivity of the carbon material (Polypropylene dispersed carbon powder) for combining to the ferrite absorber. Figure 11 shows the measured reflectivity of the double layer absorber composed the ferrite with 12 mm thick and carbon material. The resonance frequency was lower with to thicken the carbon material.

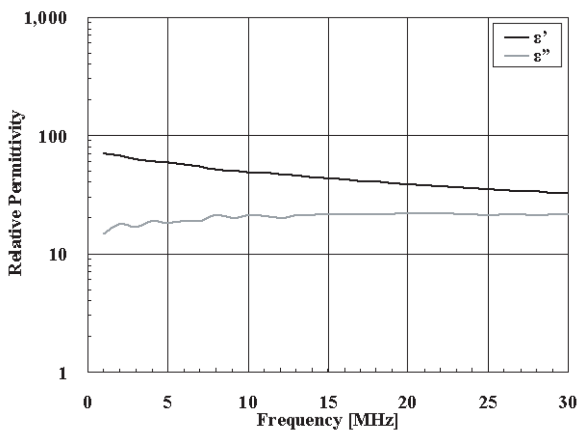

Figure 10: Relative permittivity of carbon material

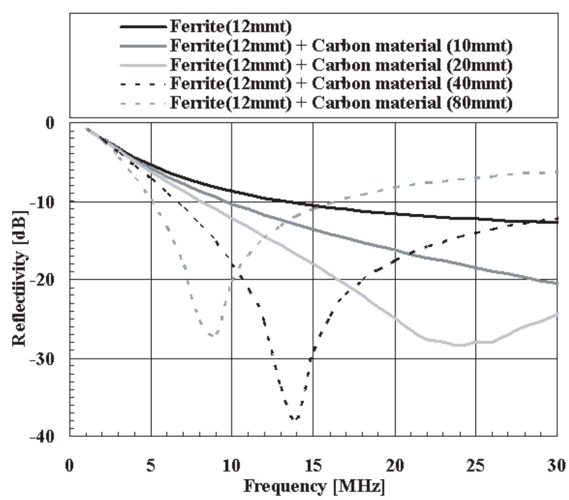

Figure 11: Reflectivity of combining carbon material.

3. Calculated Results of Site Attenuation of Semi Anechoic Chamber

Measurement layout for testing leaked E-field from PLC system is shown Figures 12 [2]. Figures 13 shows a layout of two 80 MHz tuned dipole antennas in order to calculate classical site attenuation (CSA) of a typical 3 m semi anechoic chamber lined ferrite tiles with 6.0 m wide × 9.0 m length × 5.5 m high. Test distance was 3 m, and the transmitting and the receiving antenna were each 1.5 m and 1.0 m high. The CSA of the SAC was calculated by ray tracing method, and the electro motive force (EMF) method was utilized for analysis of antenna [3]. The characteristics of the ferrite absorber which measured by the Square Coax was adopted for calculation.

Figure 14 shows the calculated of CSA of the SAC lined the ferrite tiles. To take notice of the CSA deviation of the 6.3 mm thick conventional ferrite without overlap tile, there were two large peak points at about 21 MHz and 48 MHz at horizontal polarization, and there was one large peak point at about 16 MHz at

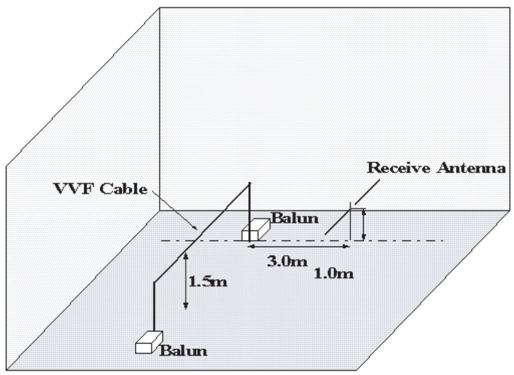

Figure 12: Layout for leaked E-field from PLC.

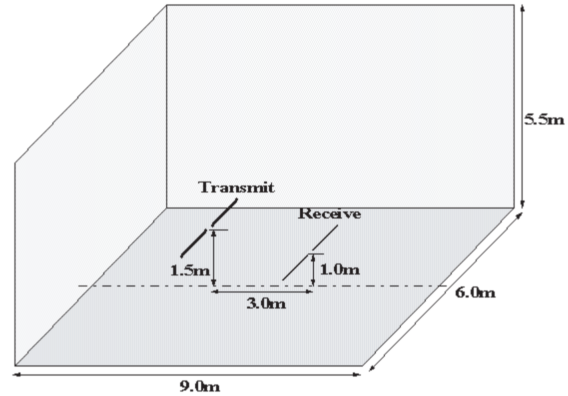

Figure 13: Model for CSA calculation of anechoic chamber.

vertical polarization. These peak points were caused by the resonance of the chamber and insufficient absorbing characteristics of the conventional ferrite absorber. The CSA deviation was reduced to put the overlap tile onto air gap between ferrite tiles. Furthermore CSA deviation was improved to about ±4 dB by adopting the double layers absorber composed the 12 mm thick ferrite tile and the 80 mm thick carbon material. The results showed that there was a possibility to evaluate PLC system in the SAC lined conventional ferrite absorber without long pyramidal absorber.

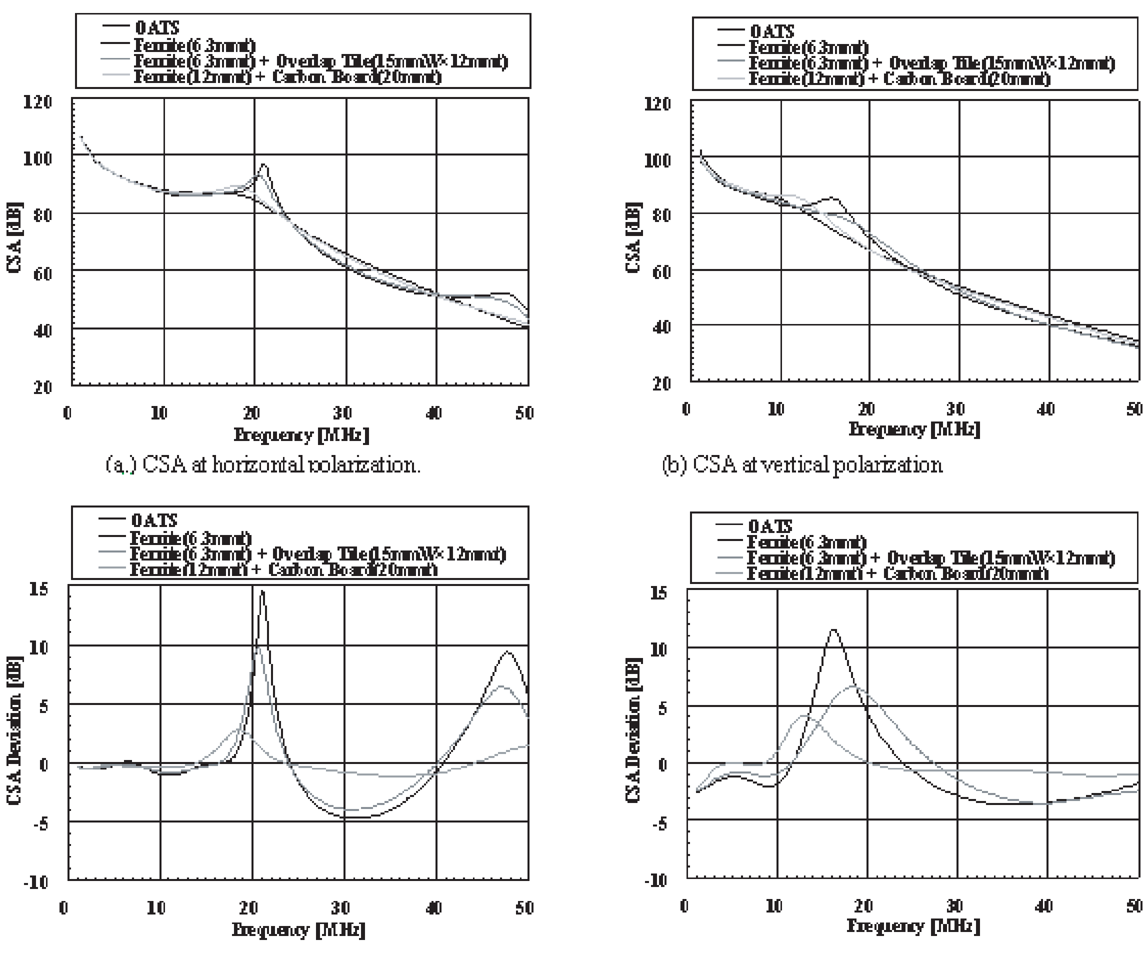

(a.) CSA at horizontal polarization.

(b) CSA at vertical polarization

(c) Deviation from CSA of OATS at horizontal polarization.

(d) Deviation from CSA of OATS at Vertical polarization.

Figure 14: Calculated CSA of semi-anechoic chamber lined conventional ferrite tiles.

4. Conclusion

The conventional ferrite absorber had not excellent absorption below 30 MHz, and it was able to improve by changing thickness of ferrite tile, adding overlap tile onto air gap or combining the carbon material with the ferrite tile. The calculated CSA deviation was improved to about ± 4 dB by adopting the double layers absorber composed the 12 mm thick ferrite tile and the 80 mm thick carbon material, it showed that there was a possibility to evaluate PLC system in the SAC lined conventional ferrite absorber without long pyramidal absorber. However the ray tracing method does not have sufficient accuracy below 100 MHz [4]. We will calculate the site attenuation by FDTD method, and will measure the actual site attenuation of the SAC which lined the conventional ferrite tiles.

REFERENCES

1. Takeya, S. and K. Shimada, "New measurement of RF absorber characteristics by large coaxial air line," *IEEE International Symposium on EMC*, 1993.
2. Watanabe, Y., M. Shiegenaga, and M. Tokuda, "Electromagnetic field near power line for a power line communication system," *International Symposium on EMC Sendai*, 2004.
3. Shimada, K. and S. Takeya, "Site attenuation calculation of ferrite chamber," *IEEE International Symposium on EMC*, 1994.
4. Kawabata, M., Y. Ishida, and K. Shimada, "Comparison of site attenuation analysis results between fdtd and ray-tracing method using compact anechoic chamber," *IEICE Trans*, Vol. E88-B, No. 8, August 2005.

Effective Medium Theory for Finite Size Aggregates

C. A. Guérin[1,2], **A. Sentenac**[1,2], **and P. Mallet**[2]

[1]Université Paul-Cézanne, France
[2]ONERA-CERT/Institut Fresnel, France

We propose an effective medium theory for random aggregates of small spherical particles which accounts for the finite size of the embedding volume. The technique is based on the identification of the successive orders of the Born series within a finite volume for the coherent field and the effective field. Although the convergence of the Born series requires a finite volume, the effective constants which are derived through this identification are shown to admit a large scale limit. With this approach we recover successively, and in a simple manner, some classical homogenization formulas: the Maxwell- Garnett (MG) mixing rule, the Effective Field Approximation, and a correction to the Quasi-crystalline Approximation (QCA) which takes into account the finiteness of the medium. The last formula will be referred to as Finite-Size Quasi-crystalline Approximation (FS-QCA). In the light of this approach, we re-examine the validity of the MG mixing rule. We show that in certain configurations MG can be accurate even at high density of scatterers or in presence of strong multiple scattering, and we give numerical evidence for this. We then discuss QCA and FS-QCA and their relationship to MG. We show that FS-QCA coincides with the usual low-frequency QCA in the limit of large volumes, while bringing substantial improvements when the dimension of the embedding medium is of the order of the probing wavelength. An application to composite spheres is proposed.

One-dimensional Modeling of Plasma-electrode Pockels Cell Driven by One-pulse Process

X. J. Zhou[1], W. Q. Guo[1, 2], X. J. Zhang[2], Z. Sui[2], and D. S. Wu[2]

[1]University of Electronic Science and Technology of China, China
[2]China Academy of Engineering Physics, China

Plasma-Electrode Pockels Cells (PEPC) are used as large-aperture optical switch in laser drivers for inertial-confinement fusion. Plasma electrodes are produced by high discharge current, while a high voltage pulse is applied across a thin KDP crystal plate through plasma, which is produced by discharge in the gas-filled cells. Gaseous ionization rises over the entire transverse section of the cells, and forms highly conductive and transparent plasma charge sheaths on the surfaces of the KDP crystal plate. In the working of PEPC in one pulse process without prior ionization of gas, the discharge plasma evolution process is time dependent. In this paper, we will present a one-dimensional modeling of processes of gaseous discharge and charging on the surfaces of KDP crystal in PEPC. Our modal is based on a simplified set of fluid equations, which is electron motion and ion motion governed by the equations of continuity and momentum conservation. The electric field distribution in the discharge cell is obtained by Poisson equation. This modeling gives the time-dependent discharge current and charging characteristics on the KDP crystal.

High Dielectric Constant Samarium Doped Barium Titanate Microwave Ceramics

D. Kaur, **S. B. Narang**, **and K. S. Thind**
Guru Nanak Dev University, India

Microwave dielectrics in ceramic form have been exploited in a variety of applications ranging from communication devices to the military satellite services. These advanced ceramics have revolutionized RF and Microwave technology. During the past decade, new material compositions developed to suit the stringent requirements for microwave resonators, filters, units of various UHF devices, substrate elements and IC packaging applications. The major advantages of microwave ceramics include the high dielectric constant (ε') and low tangent loss ($\tan\delta$) for stimulating the miniaturization and selectivity of components. The high technology dielectrics with new ideas and designs will be the basis for continuing usage of microwave ceramics in the third generation of Wireless and Telecommunication. This presentation addresses some results of investigations of the dielectric properties and the structure of ceramics based on the $BaO - Sm_2O_3 - TiO_2$ ternary system with dielectric constant greater than 70 and tangent loss less than 0.009. Samples of various compounds with appropriate forms were obtained by the solid-state double sintering synthesis or by chemical co precipitation from salt solutions. The composition x was varied based on $Ba_{6-3x}Sm_{8+2x}Ti_{18}O_{54}$ molecular formula, which has been an extensively used microwave ceramic material. The dielectric properties have been observed as a function of the composition, especially the dielectric constant (ε') and tangent loss ($\tan\delta$) changed non-linearly. The dielectric dispersion has been observed at high frequencies. It has been investigated that the dispersion is basically due to the fact that beyond a certain frequency of the applied electric field the particle exchange does not follow the alternating field.